

On the Stochastic Gradient Descent and Inverse Variance-flatness Relation in Artificial Neural Networks

Xia Xiong,¹ Yong-Cong Chen,^{1,*} Chunxiao Shi,¹ and Ping Ao¹

¹*Shanghai Center for Quantitative Life Sciences & Physics Department,*

Shanghai University, Shanghai 200444, China

Abstract

Stochastic gradient descent (SGD), a widely used algorithm in deep-learning neural networks has attracted continuing studies for the theoretical principles behind its success. A recent work uncovered a generic inverse variance-flatness (IVF) relation between the variance of neural weights and the landscape flatness of loss function near solutions under SGD [Feng & Tu, PNAS 118, 0027 (2021)]. We deploy a stochastic decomposition to analyze the dynamical properties of the weights generated by SGD. The method constructs the true “energy” function under which stationary Boltzmann distribution is a correct probabilistic ensemble. The new function, different from the usual cost function, explains the IVF relation under SGD. We further verify the scaling relation identified in Feng’s work between the variance and the flatness. Our results may bridge the gap between the classical statistical mechanics and the emerging discipline of artificial intelligence, with potential to offer better algorithms for the latter.

* Corresponding author: chenyongcong@shu.edu.cn

INTRODUCTION

An artificial neural network (ANN) is a machine learning platform which simulates a human neural system. The network and the operation are arranged in a way that resembles human neurons as well as their learning process. The system includes at least three layers: an input layer, a hidden layer and an output layer. When the network has multiple hidden layers, it is called a deep neural network (DNN). Training a DNN efficiently has become a major topic in the emerging deep-learning discipline [1–3].

Most DNNs involve certain optimization which adjusts the weights connecting neurons to minimize the so-called loss function associated with the learning process [4–6]. Among them, stochastic gradient descent (SGD) is a particularly successful algorithm employed in the field. Today SGD appears in almost all deep-learning applications. Nevertheless, the full reason behind such a good outcome is still an on-going mystery. Many researchers are actively searching for the theoretical principles behind its tremendous success [7–9]. Possibly, the high degree of anisotropy on the random noises associated with SGD enables the learning process to escape from local minima en route to the best destination [10]. Significantly, there has been an increasing number of ideas that are borrowed from the classical statistical physics [11–14].

Recently Feng et al [15] studied the SGD-based dynamics and took the overall loss function as the “thermodynamic” energy function for the “physical” system. They derived the equivalent stochastic equation and performed principal component analysis (PCA) on weights during SGD optimization. The second step aimed to reduce the dimensions of complex stochastic process in accordance with their significance. The weights were then projected onto the axes of the principal components and further analyzed. The landscape of the loss function [16, 17] was characterized by its flatness in each PCA direction. In the study they found a robust inverse relation between the weight variance and the flatness of the landscape in all PCA directions. This is in striking opposite to what would follow from the Boltzmann distribution in statistical physics. Apparently, ANN systems would appear to violate a fundamental principle of physics and display what they referred to as “inverse Einstein relation”. The present work investigates such an unconventional property in details.

We start with a formalism of stochastic decomposition developed by Ao et al. [18]. The method obtains for the dynamics a Lyapunov functional which is an alternative to the cost

function and is a close analogue to the physical energy used by e.g. the Boltzmann distribution [19]. For a linear system, the driving force can be strictly decomposed into two parts, one of which leads to balance of distribution while the other gives rise to cyclic motion on the surface of constant potential function. Together they can offer, near a stable or unstable fixed point, Boltzmann-like probability distribution as well as flux-carrying stationary states without detailed balance. The method of constructing global stochastic potential has been successfully applied to a number of practical [20], in particular biological systems [21].

The covariance matrix for the dynamics is in fact inversely proportional to the energy matrix \mathbf{U} for the global potential. Such a relationship well explains the emergence of the inverse variance-flatness relation. We also verify the scaling relationship between the weight variance and flatness by explicitly analyzing the potential energy function in the linear region. Further application of stochastic decomposition in ANN may offer better algorithm, and address problems such as the well-known “forgetting” catastrophe [22, 23] while performing multi tasks.

The work is organized as follows. In the next section we clarify the IVF relation, also called the “inverse Einstein relation” for SGD-based ANN discovered by Feng et al. We then in Sect. briefly review the stochastic decomposition and identify the relationship between the covariance matrix and the potential energy matrix. In Sect. we look further into the question of IVF with respect to the Boltzmann distribution under the proper energy function. In Sect. we re-establish the scaling relationship between variance and flatness via the new approach. Finally, we conclude with some discussions and an outlook to the algorithm optimization in ANN.

THE INVERSE VARIANCE-FLATNESS RELATION

Following Feng et al [15], in the continuous-time limit [24] SGD can be cast into a conventional set of stochastic differential equation

$$\dot{\boldsymbol{\omega}} = -\alpha \nabla_{\boldsymbol{\omega}} L(\boldsymbol{\omega}) + \boldsymbol{\eta}(t). \quad (1)$$

We shall throughout the work use boldface for matrix or vector, while the same symbol in normal face for the underlying matrix element. In Eq. (1) $\boldsymbol{\omega}$ is an array of weights in question (a state vector), α is a learning rate, $\dot{\boldsymbol{\omega}} \equiv d\boldsymbol{\omega}/dt$, and $L(\boldsymbol{\omega})$ is an overall loss function for the

learning process. Note that L was incorrectly regarded in [15] as the energy function for the stochastic system, a key point that will be heavily emphasized below. The SGD noise term $\boldsymbol{\eta} \equiv -\alpha \nabla_{\boldsymbol{\omega}}(L^\mu - L)$ arises from the variation between a mini-batch loss function (MLF) $[L^\mu(\boldsymbol{\omega})$ for the μ^{th} batch picked at the time $t]$ and its ensemble average, with $\langle \boldsymbol{\eta} \rangle_\mu = 0$ but non-zero variance $\langle \eta_i(t) \eta_j(t') \rangle_\mu$ for $t = t'$.

We next summarize the main result obtained by Feng et al [15]. After carrying out PCA on the SGD process, the weight dynamics can be projected out for variations in the principal components $\boldsymbol{\omega}(t) = \langle \boldsymbol{\omega} \rangle_T + \sum_i^N \theta_i(t) \mathbf{p}_i$. Here $\langle \boldsymbol{\omega} \rangle_T \equiv \boldsymbol{\omega}_0$ is the average weight vector in a particular epoch time of length T , \mathbf{p}_i is the i^{th} principal component base vector and the projection on the PCA direction \mathbf{p}_i is given by $\theta_i(t)$. Let the loss function profile along \mathbf{p}_i be $L_i(\delta\theta) \equiv L(\boldsymbol{\omega}_0 + \delta\theta \mathbf{p}_i)$. Numerous data simulations found that L_i tends to be flatter with the increase of i .

To quantify the property, a flatness parameter can be introduced as follows[25–27]. $F_i = \theta_i^r - \theta_i^l$ ($\theta_i^l < 0, \theta_i^r > 0$) is taken as the difference between the nearest two points ($L_i(\theta_i^l) = L_i(\theta_i^r) = e \times L_0$) of equal value near the minimum found by SGD. Now F_i is found to increase with PCA direction i , while the SGD variance σ_i^2 decreases with i by definition. The result is counter-intuitive: When the landscape of the “energy function” is deep, the stochastic process shows large variance. Namely, the flatter the “energy function” the less diffusive the dynamics. Finally the variance-flatness relation follows approximately a power-law behavior,

$$\sigma_i^2 \sim F_i^{-4}. \quad (2)$$

To illustrate the key point further, the above stands in stark contrast to conventional statistical physics as the latter would state that the equilibrium probability takes the form of Boltzmann distribution $P(\boldsymbol{\theta}) = \exp[-L(\boldsymbol{\theta})/T]$ (with T characterizing the “thermal” fluctuations). With the distribution the variance of θ_i would be proportional to F_i^2 . But the opposite phenomenon, the IVF is observed in Eq. (2), which is also referred to as the “inverse Einstein relation” in [15]. Such property appears to violate the basic principle of statistical physics.

COVARIANCE MATRIX OF THE STOCHASTIC DYNAMICS

Feng’s work utilized the well-known PCA technique in which covariance of stochastic process plays a pivot role in the whole analysis [28]. We next introduce an alternative method of stochastic decomposition and show how it is inherently related to the covariance matrix. In doing so we gain a crucial relationship between the covariance and the “true” energy function that can be used in the Boltzmann distribution, fulfilling a major goal of the present work.

A Review of the Stochastic Decomposition

A large class of stochastic processes in nature can be modeled by the following set of stochastic differential equations (SDE) [29],

$$\dot{\mathbf{x}} = f(\mathbf{x}) + \boldsymbol{\zeta}(t), \quad (3)$$

where \mathbf{x} stands for the state vector of a N -dimensional system. Here $f(\mathbf{x})$ and $\boldsymbol{\zeta}(t)$ are respectively the deterministic and a Markovian driving force for the dynamics. In many cases $\boldsymbol{\zeta}(t)$ can be represented by a Gaussian white noise with $\langle \boldsymbol{\zeta}(t) \rangle = 0$ and semi-positive definite variance $\langle \boldsymbol{\zeta}(t) \boldsymbol{\zeta}^\tau(t') \rangle = 2\epsilon \mathbf{D} \delta(t - t')$. The superscript τ denotes the transpose of the underlying vector/matrix, $\langle \dots \rangle$ is the average over the Gaussian distribution, and $\delta(t)$ is the Kronecker delta function for the Markovian process. Evidently \mathbf{D} is a diffusion matrix and ϵ the noise strength, which plays the role of temperature arising from the stochasticity. For the analysis below, we will focus on dynamics near a fixed point so that the first term in Eq. (3) may be approximated by $f_i(x) = -F_{ij}x_j$. Namely, equation reduces to

$$\dot{\mathbf{x}} = -\mathbf{F}\mathbf{x} + \boldsymbol{\zeta}(t). \quad (4)$$

The aforementioned stochastic decomposition seeks to re-cast the dynamics into the following “canonical” form,

$$(\mathbf{S} + \mathbf{A}) \dot{\mathbf{x}} = -\mathbf{U}\mathbf{x} + \boldsymbol{\xi}(t). \quad (5)$$

Among the terms \mathbf{U} is a symmetric potential matrix which gives rise to an energy function for the whole system $u(\mathbf{x}) = \mathbf{x}^\tau \mathbf{U} \mathbf{x} / 2$. \mathbf{S} is symmetric, semi-positive definite. It represents the dissipative dynamics which in the absence of fluctuations causes monotonic decrease of

$u(\mathbf{x})$. The canonical noise $\boldsymbol{\xi}$ is associated with \mathbf{S} by a generalized fluctuation-dissipation theorem $\langle \boldsymbol{\xi}(t) \boldsymbol{\xi}^\tau(t') \rangle = 2\epsilon \mathbf{S} \delta(t - t')$. On the other hand, \mathbf{A} is antisymmetric and conserves $u(\mathbf{x})$. With the canonical form and the knowledge of the potential, it can be shown that [18] the Boltzmann-like distribution

$$\rho(\mathbf{x}) \propto \exp\{-u(\mathbf{x})/\epsilon\} \quad (6)$$

presents a stationary distribution for the state variable. That is, the potential function so constructed bears the essence of energy in statistical physics.

Going back to Eq. (4), the two norms of noises are related by

$$\boldsymbol{\xi}(t) = (\mathbf{S} + \mathbf{A}) \boldsymbol{\zeta}(t). \quad (7)$$

Hence \mathbf{S} is related to the diffusion matrix \mathbf{D} by

$$\mathbf{S} = (\mathbf{S} + \mathbf{A}) \mathbf{D} (\mathbf{S} - \mathbf{A}). \quad (8)$$

To make further connection, we look at the inverse of $(\mathbf{S} + \mathbf{A})^{-1}$ and break it down to symmetric $\tilde{\mathbf{D}}$ and anti-symmetric \mathbf{Q} . It turns out $\tilde{\mathbf{D}}$ satisfies the same equation as \mathbf{D} does in Eq. (8) and $(\mathbf{S} + \mathbf{A}) \mathbf{Q} (\mathbf{S} - \mathbf{A}) = -\mathbf{A}$.

To obtain the potential function, we rewrite the force matrix \mathbf{F} as

$$\mathbf{F} = (\mathbf{S} + \mathbf{A})^{-1} \mathbf{U} = (\mathbf{D} + \mathbf{Q}) \mathbf{U}. \quad (9)$$

Then according to the symmetry of \mathbf{U} , \mathbf{D} and \mathbf{Q} , \mathbf{Q} and \mathbf{U} can be determined uniquely from \mathbf{F} and \mathbf{D} by

$$\mathbf{F} \mathbf{Q} + \mathbf{Q} \mathbf{F}^\tau = \mathbf{F} \mathbf{D} - \mathbf{D} \mathbf{F}^\tau, \quad (10)$$

$$\mathbf{F} \mathbf{U}^{-1} + \mathbf{U}^{-1} \mathbf{F}^\tau = 2\mathbf{D}. \quad (11)$$

The above analysis holds at least near a stable fixed point where real parts of eigenvalues of \mathbf{F} are positive, a condition that is assumed to be satisfied in what follows. Further details can be found in e.g. [19].

Evaluation of Covariance Matrix

To proceed further we solve Eq. (4) for the system as,

$$\mathbf{x}(t) = e^{-\mathbf{F}t} \left[\mathbf{x}(0) + \int_0^t e^{\mathbf{F}t'} \boldsymbol{\zeta}(t') dt' \right]. \quad (12)$$

The covariance is calculated from normalized \mathbf{x} with zero means. Namely, $\tilde{\mathbf{x}}(t) = \mathbf{x}(t) - (1/t) \int_0^t \mathbf{x}(t') dt'$. Near a stable fixed point the homogeneous part decays exponentially. Therefore at $t \rightarrow \infty$ the covariance matrix Σ can be readily obtained as

$$\Sigma = \langle \tilde{\mathbf{x}}(t) \tilde{\mathbf{x}}^\tau(t) \rangle_{t \rightarrow \infty} = 2 \int_{-\infty}^0 dt e^{\mathbf{F}t} \mathbf{D} e^{\mathbf{F}^\tau t}. \quad (13)$$

The integration can be further carried out [30] to get

$$\mathbf{F}\Sigma + \Sigma\mathbf{F}^\tau = 2\epsilon \int_{-\infty}^0 dt \frac{d}{dt} [e^{\mathbf{F}t} \mathbf{D} e^{\mathbf{F}^\tau t}] = 2\epsilon \mathbf{D}. \quad (14)$$

It follows from Eq. (11) that the covariance matrix and the potential energy matrix are the mutual inverse of each other

$$\Sigma = \epsilon \mathbf{U}^{-1}. \quad (15)$$

Therefore, the largest principal components of Σ correspond to the eigenstates of \mathbf{U} with smallest eigenvalues.

BOLTZMANN DISTRIBUTION OF NEURAL WEIGHTS

We have identified a special relationship between the loss function and the stochastic potential, which suggests that the IVF mystery may be traced back to the choice of the energy function. In an ANN, if the loss function was incorrectly assumed as the energy function, the relationship between variance and flatness would not conform from the usual Boltzmann distribution. Instead, they showed the counter-intuitive IVF characteristic.

The proper Boltzmann distribution should follow when the stochastic potential is employed. Since $\mathbf{U} \sim \Sigma^{-1}$, a larger covariance matrix corresponds to a smaller potential energy matrix. In terms of the projection on the eigenvectors, the value of variance reduces as the eigenvalue of \mathbf{U} increases. The stochastic potential $u(\mathbf{x}) = \mathbf{x}^\tau \mathbf{U} \mathbf{x} / 2$ is a quadratic function, its landscape becomes flatter as the \mathbf{U} decreases, leading to larger F_i . Hence, there is a positive correlation between the variance and the ‘‘correct’’ flatness, contrary to what appears in Eq. (2).

For a clear comparison, we have summarized the various relationships in Fig. 1 with a graphic illustration. The loss function landscape exhibits a flatter behavior as i , index of the PCA axes increases. However, the opposite is observed on the stochastic potential. On a preliminary analysis where the off-diagonal matrix elements are ignored, the loss function has

roughly an inverse relationship to the stochastic potential. A flat landscape of loss function corresponds to a steep trap on the stochastic potential. When data simulations yield results which associate larger variance to steeper loss function, they actually correspond to flatter stochastic landscape. Such a feature is precisely what the Boltzmann distribution from the latter will present.

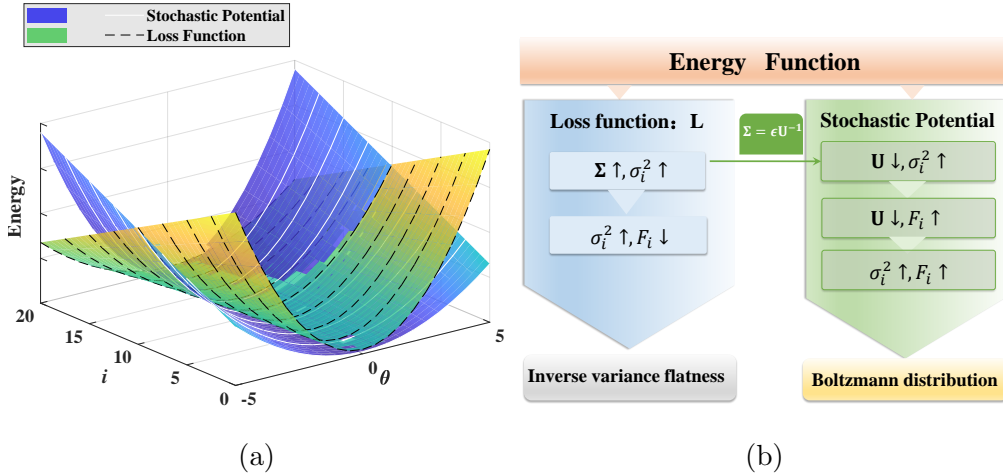


FIG. 1. A summary of relationships among the stochastic potential, the loss function, the variance and the flatness. (a) A schematic plot of the variations of stochastic potential and loss function on the PCA index i . (b) The choice of energy function, either the loss function or the stochastic potential leads to different observations. Legends: Σ – covariance matrix; σ_i^2 – variance; \mathbf{U} – potential matrix; F_i – flatness; ϵ – noise strength; \uparrow, \downarrow – moments of the values.

ESTIMATE OF THE SCALING BEHAVIOR

The stochastic potential well explains the emergence of the IVF relation and resolve the conceptual difficulty. To further elaborate on the usefulness of the stochastic potential, we now study the characteristic of the diffusion matrix. It is then used to verify the scaling relationship between the variance and the flatness (defined via the loss function).

Diffusion Approximation of SGD

An ANN optimizes its state vector, i.e. weights and biases through a learning process. In general, the loss function can be rather complex and the parameter space is huge [31–33].

On a gradient descent scheme, the state vector advances a certain step from the current position along the opposite direction of the gradient. The latter is re-calculated at the new position to continue the movement. When the data used for training are randomly selected mini batches, the scheme is known as SGD, the stochastic gradient descent [34, 35]. In this case, the state vector is updated via

$$\omega_{k+1} = \omega_k - \alpha \nabla_{\omega} L^{\mu}(\omega), \quad (16)$$

where α is a learning rate, and $\nabla_{\omega} L^{\mu}(\omega)$ is the gradient over the μ^{th} mini-batch of size B . The stochastic equation in the continuous-time limit is given by Eq. (3). After PCA projection, the dynamics of weights is represented by $\boldsymbol{\theta}$ as

$$\dot{\boldsymbol{\theta}} = -\alpha \nabla_{\boldsymbol{\theta}} L(\boldsymbol{\theta}) + \boldsymbol{\eta}(t), \quad (17)$$

cf. Eq. (1) for more explanations.

To link Eq. (17) to Eq. (4), we need knowledge on the noise variance $\langle \eta_i(t) \eta_j(t') \rangle \propto \alpha^2 \langle \nabla_{\theta_i}(L^{\mu} - L) \nabla_{\theta_j}(L^{\mu} - L) \rangle \delta(t - t')$. Note that the leaning set is assumed to be sufficiently large so that there is no correlations between the mini batches. In the SGD process when a mini-batch is sampled with replacement, the variance is approximately [10]

$$\langle (\nabla L^{\mu} - \nabla L)(\nabla L^{\mu} - \nabla L) \rangle_{\mu} \approx \mathbf{D}(\boldsymbol{\theta})/B, \quad (18)$$

where $\mathbf{D}(\boldsymbol{\theta})$ is a diffusion matrix independent of the mini batches,

$$\mathbf{D}(\boldsymbol{\theta}) \approx \left(\frac{1}{N_L} \sum_{k=1}^{N_L} \nabla L_k(\boldsymbol{\theta}) \nabla L_k(\boldsymbol{\theta}) \right) - \nabla L(\boldsymbol{\theta}) \nabla L(\boldsymbol{\theta}), \quad (19)$$

where N_L is the total size of the learning set. Evidently, the noise strength ϵ in Eq. (6) to scales to α^2/B .

To go further from the generic presentation, we follow Feng et. al. [15] but truncate the MLF L^{μ} to a quadratic function near its minimum,

$$L^{\mu}(\boldsymbol{\theta}) \approx L_0^{\mu} \left\{ \sum_i \frac{M_{ii}^{\mu}}{2} \theta_i (\theta_i - 2\theta_i^{\mu}) + \sum_{i < j} M_{ij}^{\mu} (\theta_i \theta_j - \theta_i \theta_j^{\mu} - \theta_j \theta_i^{\mu}) \right\}. \quad (20)$$

The model has a simple “physical” interpretation. For the μ^{th} mini batch, the system evolves towards an attractor $\boldsymbol{\theta}^{\mu}$, the location of minimum cost function for the μ^{th} batch;

$\mathbf{M}^\mu = \{M_{ij}^\mu\}$ is a symmetric Hessian matrix. These random variables are assumed to be un-correlated and obey the normal distributions, i.e. $M_{ii}^\mu \sim N(M_{ii}^{(0)}, \sigma_{M,i}^2)$, $M_{ii}^{(0)} > 0$; $M_{ij}^\mu \sim N(0, \sigma_{ij}^2)$, $i \neq j$; $\theta_i^\mu \sim N(0, \sigma_{\theta,i}^2)$, $i > 1$; $\theta_1^\mu \sim N(\theta_1^{(0)}, \sigma_{\theta,1}^2)$. Note that $i = 1$ has a special place in the analysis, which is associated with the drifting of the minimum discussed in details in [15]. The simplification allows us to obtain the overall loss function as

$$\begin{aligned} L(\boldsymbol{\theta}) &\equiv \langle L^\mu(\boldsymbol{\theta}) \rangle_\mu \approx \left\langle L_0^\mu \left\{ \sum_i \frac{M_{ii}^\mu}{2} \theta_i (\theta_i - 2\theta_i^\mu) \right. \right. \\ &\quad \left. \left. + \sum_{i < j} M_{ij}^\mu (\theta_i \theta_j - \theta_i \theta_j^\mu - \theta_j \theta_i^\mu) \right\} \right\rangle_\mu \\ &\approx L_0 \left(-M_{11}^{(0)} \theta_1^{(0)} \theta_1 + \sum_{i > 1} \frac{M_{ii}^{(0)}}{2} \theta_i^2 \right), \end{aligned} \quad (21)$$

where

$$M_{ii} \approx M_{ii}^{(0)}. \quad (22)$$

The elements of the diffusion matrix can be expressed as

$$D_{ij} \approx \langle \nabla_{\theta_i} L^\mu \nabla_{\theta_j} L^\mu \rangle_\mu - \nabla_{\theta_i} L^\mu \nabla_{\theta_j} L^\mu. \quad (23)$$

For the analysis below we will only focus on the diagonal elements, i.e. dropping the correlations between different principal axes,

$$D_{ii} \approx L_0^2 (M_{ii}^{(0)})^2 \sigma_{\theta,i}^2. \quad (24)$$

Scaling Analysis

Going back to the stochastic decomposition for the SGD equation, the first term on the right-hand side of Eq. (4) is equivalent to that in Eq. (17)

$$-F_{ii} \theta_i \approx -\alpha L_0 M_{ii}^{(0)} \theta_i. \quad (25)$$

Namely, $\alpha L_0 M_{ii}^{(0)}$ is the diagonal value of the force matrix \mathbf{F} . Since $M_{ii}^{(0)} \sim F_i^{-2}$ (by definition of flatness), the same scaling applies for the force matrix, $F_{ii} \sim F_i^{-2}$.

The diffusion coefficient D_{ii} obtained here is similar to Eq. 12 of Feng [15]. In their work D_{ii} was divided into two factors and the first one goes as $(M_{ii}^{(0)})^2 \sim F_i^{-4}$. But they got the second one, according to data simulations as $\sigma_{\theta,i} \sim F_i$ (cf. FIG. S6 of [15]). In the process

of identifying the second scaling property, they chose to fix the PCA axis and looked at the behavior between different time windows as it approaches the minimum. This is, we strongly believe, erroneous. What should be analyzed is the scaling behavior upon varying the PCA index i itself.

To make a rough estimate of the appropriate scaling property, we go back to Eq. (19), the expression for the diffusion matrix. It is easy to realize that the important contribution arises from the regions where the loss function is steep. This is where the first term in Eq. (19) overpower second term in magnitude. Based on this observation, we expect $\mathbf{D} \sim \mathbf{F}^n$ with $n > 2$. Since $F_{ii} \sim F_i^{-2}$, we have $D_{ii} \sim F_i^{-2n}$. Taking $n \approx 3$ implies that, from Eq. (24) $\sigma_{\theta,i}^2 \sim F_i^{-2}$, an inverse relationship to what was found in [15]. The reversed scaling behavior is much more reasonable as one does not expect that $\sigma_{\theta,i}^2$ and σ_i^2 behave totally the opposite way. Finally, substituting $D_{ii} \sim F_i^{-6}$ into Eq. (14), we get $\Sigma_{ii} = \sigma_i^2 \sim F_i^{-4}$. This recovers the same scaling behavior as that obtained from data simulations in [15].

DISCUSSIONS

This work aims to resolve the IVF dilemma found in ANNs optimized under SGD algorithm. It reveals the non-equivalence of loss function to the energy function when the dynamics is considered in the context of statistical physics. Instead, a stochastic potential rising from a stochastic decomposition procedure may be used as the energy function. The procedure incorporates the properties of the associated stochasticity under the generalized fluctuation-dissipation framework. With the proper energy function, there is no apparent violation of physical principles.

Then how much the two functions resemble each other? Chaudhari et al. [10] showed through some rigorous proof that the energy is related to the loss function but not necessarily equal to the latter. They are the same if and only if the noise of the mini-batch gradient is isotropic. Nevertheless the noise in a SGD-driven system is in general highly anisotropic, which leads to the IVF relation observed in data simulations.

The anisotropy of the noise appears highly desirable. It allows the system to skip local minima en route to a better global solution. As a result it performs well in training real-life neural networks. In an effort to understand the principle behind SGD, many studies on SGD have been carried out. To this end, we propose to construct the stochastic potential,

an energy function that is closely related to the noise, through a stochastic decomposition framework. The IVF phenomenon can be further elaborated. In particular the scaling property so obtained is consistent with that from data simulations. These successes are indications that our method can be well adopted in ANN studies.

The stochastic decomposition itself can reveal rich structural features. In a related study [36], the eigenvalues and eigenvectors of the \mathbf{S} and \mathbf{A} matrices [cf. Eq. (5)], are very characteristic. Assuming that we find a way to re-scale the noises back to isotropy, then the eigenstates of \mathbf{S} can be expressed as the direct sum of multiple matrices, $\mathbf{S} = \mathbf{s}_1 \oplus \mathbf{s}_2 \oplus \dots \mathbf{s}_{N/2}$, where $\mathbf{s}_i = s_i \mathbf{1}$. Here, $s_i > 0$ is the i^{th} eigenvalue which can be labelled by $s_1 \leq s_2 \leq s_2 \leq \dots \leq s_{N/2}$ and $\mathbf{1}$ is the 2×2 unit matrix. Similarly, in the same subspaces \mathbf{A} can be diagonalized into a direct sum of pairs of 2×2 antisymmetric matrices. The system is often found to be circulating in one of the subspaces, i.e. a vortex-like behavior.

The above characteristic may be useful for a trial solution of the catastrophic weight-forgetting difficulty. The latter refers to the problem when a neural network learns a new task under the premise that it has already learned an old one, the system often performs poorly on the first task afterwards. This can be due to heavy shifting of weight parameters so that the old settings are forgotten [22]. It is possible that vortices identified above can be used to pin-down the shifting and multiple tasks can be assigned to different vortices. These ideas may be beneficial to future algorithm development.

This work was supported in part by the National. Natural Science Foundation of China No. 16Z103060007 (PA). One of us (XX) thanks Dr. Pratik Chaudhari for the communications and free codes from his work.

-
- [1] Y. LeCun, Y. Bengio, and G. Hinton, *Nature* **521**, 436 (2015).
 - [2] I. Goodfellow, Y. Bengio, and A. Courville, *Deep Learning* (MIT Press, 2016).
 - [3] C. C. Aggarwal, *Neural Networks and Deep Learning* (Springer Press, 2018).
 - [4] Q. V. Le, J. Ngiam, A. Coates, A. Lahiri, B. Prochnow, and A. Y. Ng, in *Proceedings of the 28th International Conference on International Conference on Machine Learning* (2011) pp. 265—272.
 - [5] J. Martens *et al.*, in *Proceedings of the 27th International Conference on International Con-*

- ference on Machine Learning* (2010) pp. 735–742.
- [6] S. R. Young, D. C. Rose, T. P. Karnowski, S.-H. Lim, and R. M. Patton, in *Proceedings of the Workshop on Machine Learning in High-performance Computing Environments* (2015) pp. 1–5.
 - [7] M. Advani, S. Lahiri, and S. Ganguli, *Journal of Statistical Mechanics: Theory and Experiment* **2013**, P03014 (2013).
 - [8] C. Baldassi, C. Borgs, J. T. Chayes, A. Ingrosso, C. Lucibello, L. Saglietti, and R. Zecchina, *Proceedings of the National Academy of Sciences* **113**, E7655 (2016).
 - [9] C. Zhang, S. Bengio, M. Hardt, B. Recht, and O. Vinyals, *Communications of the ACM* **64**, 107 (2021).
 - [10] P. Chaudhari and S. Soatto, in *2018 Information Theory and Applications Workshop* (2018) pp. 1–10.
 - [11] Y. Zhang, A. M. Saxe, M. S. Advani, and A. A. Lee, *Molecular Physics* **116**, 3214 (2018).
 - [12] Y. Feng and Y. Tu, *Machine Learning: Science and Technology* **2**, 043001 (2021).
 - [13] G. Carleo, I. Cirac, K. Cranmer, L. Daudet, M. Schuld, N. Tishby, L. Vogt-Maranto, and L. Zdeborová, *Reviews of Modern Physics* **91**, 045002 (2019).
 - [14] P. Mehta, M. Bukov, C.-H. Wang, A. G. Day, C. Richardson, C. K. Fisher, and D. J. Schwab, *Physics Reports* **810**, 1 (2019).
 - [15] Y. Feng and Y. Tu, *Proceedings of the National Academy of Sciences* **118**, e2015617118 (2021).
 - [16] B. Ghorbani, S. Krishnan, and Y. Xiao, in *Proceedings of the 36th International Conference on Machine Learning* (Proceedings of Machine Learning Research, 2019) pp. 2232–2241.
 - [17] H. Li, Z. Xu, G. Taylor, C. Studer, and T. Goldstein, *Advances in Neural Information Processing Systems* **31** (2018).
 - [18] P. Ao, *Journal of Physics A: Mathematical and General* **37**, L25 (2004).
 - [19] C. Kwon, P. Ao, and D. J. Thouless, *Proceedings of the National Academy of Sciences* **102**, 13029 (2005).
 - [20] Y.-C. Chen, C. Shi, J. M. Kosterlitz, X. Zhu, and P. Ao, *Proceedings of the National Academy of Sciences* **117**, 23227 (2020).
 - [21] R. Yuan, X. Zhu, G. Wang, S. Li, and P. Ao, *Reports on Progress in Physics* **80**, 042701 (2017).
 - [22] A. Robins, *Connection Science* **7**, 123 (1995).

- [23] J. Kirkpatrick, R. Pascanu, N. Rabinowitz, J. Veness, G. Desjardins, A. A. Rusu, K. Milan, J. Quan, T. Ramalho, A. Grabska-Barwinska, *et al.*, [Proceedings of the National Academy of Sciences](#) **114**, 3521 (2017).
- [24] H. Sompolinsky, A. Crisanti, and H.-J. Sommers, [Physical Review Letters](#) **61**, 259 (1988).
- [25] S. Hochreiter and J. Schmidhuber, [Neural Computation](#) **9**, 1 (1997).
- [26] P. Chaudhari, A. Choromanska, S. Soatto, Y. LeCun, C. Baldassi, C. Borgs, J. Chayes, L. Sagun, and R. Zecchina, [Journal of Statistical Mechanics: Theory and Experiment](#) **2019**, 124018 (2019).
- [27] C. Baldassi, F. Pittorino, and R. Zecchina, [Proceedings of the National Academy of Sciences](#) **117**, 161 (2020).
- [28] H. Abdi and L. J. Williams, [Wiley Interdisciplinary Reviews: Computational Statistics](#) **2**, 433 (2010).
- [29] N. G. Van Kampen, *Stochastic Processes in Physics and Chemistry* (VElsevier Press, 1992).
- [30] M. Han, J. Park, T. Lee, and J. H. Han, [Physical Review E](#) **104**, 034126 (2021).
- [31] A. J. Bray and D. S. Dean, [Physical Review Letters](#) **98**, 150201 (2007).
- [32] R. D. Beer, [Neural Computation](#) **18**, 3009 (2006).
- [33] S.-i. Amari, [Advances in Neural Information Processing Systems](#) **9** (1996).
- [34] M. Rattray, D. Saad, and S.-i. Amari, [Physical Review Letters](#) **81**, 5461 (1998).
- [35] J. Sohl-Dickstein, B. Poole, and S. Ganguli, in *Proceedings of the 31st International Conference on Machine Learning* (Proceedings of Machine Learning Research, 2014) pp. 604–612.
- [36] Y.-C. Chen, C. Shi, J. M. Kosterlitz, X. Zhu, and P. Ao, [Proceedings of the National Academy of Sciences](#) (submitted).